IOP Conf. Series: Journal of Physics: Conf. Series **881** (2017) 012018 doi:10.1088/1742-6596/881/1/012018

Possibilities of the mirror through transmission electromagnetic-acoustic technique on multiple reflections

K V Petrov, O V Muravieva, M A Gabbasova and V A Zorin

Kalashnikov Izhevsk State Technical University, 7 Studencheskaia Str., 426069 Izhevsk, Russia

E-mail: kirillpetr@list.ru

Abstract. The approaches to the implementation of the mirror through transmission electromagnetic-acoustic (EMA) testing technique on multiple reflections are introduced. Operating principles of through-type EMA transducers and the special-purpose installation realizing the mirror through transmission EMA testing technique on multiple reflections are described. The modeling results of electrodynamic mechanism of interaction between the through type EMA transducers are presented and used for the efficiency increase and the improvement of dimensional characteristics. The special model, with the use of which the formation principles of through-type EMA transducer acoustic fields in cylindrical objects were investigated, is developed. The additional informative parameters based on the correlation, spectral and probability and statistic analyses of the multiple reflections oscillograms are suggested. The results of structural analysis and investigation of acoustoelasticity with the use of the mirror through transmission EMA technique on the multiple reflections are presented.

1. Introduction

Acoustic, magnetic, eddy current and optical types of nondestructive testing are used to control cylindrical objects (rods and products made of them such as shafts, pump rods, rollers and others). Magnetic, eddy current and optical techniques allow detecting only surface and subsurface defects, while it is possible to detect both surface and internal defects of the cylindrical objects by acoustic techniques. Feature of testing of the cylindrical objects with small diameters is difficulty of realization of traditionally used contact ultrasound techniques, veracity and repeatability of which depend on surface finish quality of the testing objects and their diameters.

The mirror through transmission electromagnetic-acoustic (EMA) technique on multiple reflections is suggested by the authors for testing of cylindrical objects. Advantages of the suggested technique include non-contact nature of excitation and reception of ultrasound waves, possibility of excitation and reception of any kinds of waves, high sensitivity during stress-strain behavior estimation, structural analysis, thickness measurement and non-destructive testing due to the use of multiple reflections, ability to work under low and high temperatures and on rough and foul object surface [1-4]. Disadvantage of this technique is a low EMA conversion coefficient, which requires the search of new technical solutions on development of bias system, generators of powerful probing pulses, low-noise receiving and amplifying path with a wide dynamic range.

Content from this work may be used under the terms of the Creative Commons Attribution 3.0 licence. Any further distribution of this work must maintain attribution to the author(s) and the title of the work, journal citation and DOI.
Published under licence by IOP Publishing Ltd

The results of numerical modeling of EMA transducer acoustic and electromagnetic fields with the purpose of bias system optimization and acoustic field analysis are presented in the article. The possibilities of the developed technique with the use of body and Rayleigh waves are shown for quality control of the cylindrical objects, including flaw detection, structural analysis, estimation of elastic moduli, anisotropy and metal stress-strain behavior and measurement of diameter deviation and rod cross section ellipticity.

2. Technique realization

The suggested technique is realized with the special-purpose through-type EMAT of the body waves (figure 1) and laid-on EMAT of Rayleigh waves. The use of the through type EMA transducers provides radiation and reception of compressional and shear waves with axial polarization in all radial directions over rod cross section. The laid-on EMA transducer provides radiation and reception of the Rayleigh waves along rod perimeter with elliptic polarization. (figure 2).

Figure 1. The through type EMAT for testing of the rods with diameter of 44 mm.

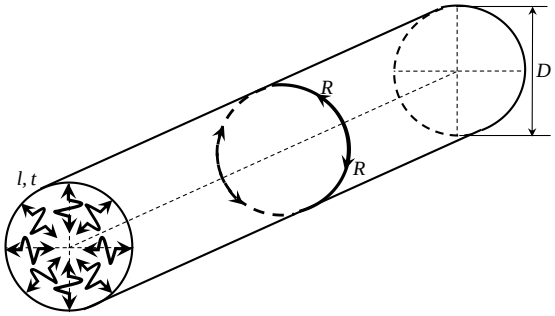

Figure 2. Propagation concept of compressional *l* and shear *t* waves with radial directions along the cross section and Rayleigh waves *R* along rod envelope.

The flow chart of the installation is illustrated in figure 3. The installation operates as described further. The probe pulse generator generates a powerful electrical signal with amplitude up to 1.5 kV, which is transferred to the EMAT and converted to the ultrasound pulse propagating in the testing object. The multiply reflected ultrasound pulse is received by the same EMAT, filtered by a bandpass filter and transferred to an amplifier with an amplifying coefficient of 76 dB in the frequency bandwidth from 1 to 4 MHz. The amplified signal comes to an analog-to-digital converter (ADC) with a sampling frequency of 100 MHz, which converts the received signal to the digital form for the further visualization and processing on a personal computer (PC) with special software.

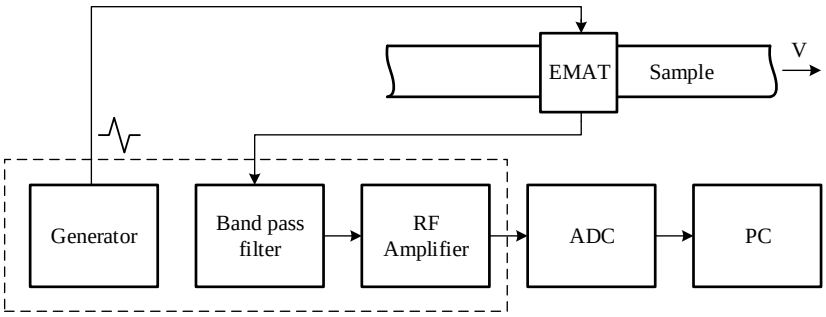

Figure 3. The flow chart of EMA installation.

The pulse series of multiple reflections of body *l* and *t* waves along the rod diameter and flow-through pulses of the Rayleigh *R* waves multiply passed over the rod perimeter in forward and backward directions are observed on the screen of defectoscope (figure 4). The registration and estimation of the received signals is carried out with the use of the special- purpose software «Prince» [5]. The high sampling frequency of analog-to-digital conversion, possibility of obtaining the multiple reflection series and further interpolation provide high accuracy of wave velocity measurement (0.05%).

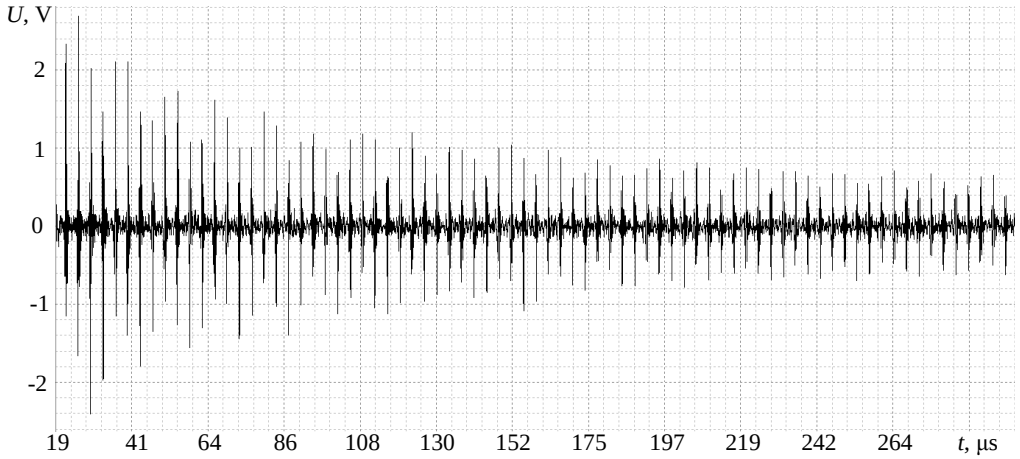

Figure 4. The oscillogram of the multiple reflection series obtained during testing.

3. Modeling of magnetic, eddy current and acoustic fields of EMAT

The electromagnetic-acoustic transducer consists of a special bias system and a high-frequency inductor. The excitation of the acoustic wave happens due to the electrodynamic mechanism of interaction between eddy currents *i*, caused by alternating current of the high-frequency inductor with length *dl* and the constant magnetic field B_0 and presence of Ampere force:

$$F_A = i_в \left[dl \cdot B_0 \right]. \quad (1)$$

Ampere forces F_A are formed in subsurface layer of the testing object:

$$\delta = \sqrt{2/\omega\mu_0\mu\sigma}\,, \quad (2)$$

where $\mu_0=4\pi\cdot10^{-7}$ H/m, μ is a relative magnetic permeability, σ is an electrical conductivity, $\omega=2\pi f$ is a wave circular frequency.

The acoustic wave pulses are received by the same transducer due to the converse mechanism where the electromagnetic fields caused by eddy currents *j* in subsurface layer of the object, fluctuating with the velocity *V* in a bias field with induction B_0, are registered by the high-frequency inductor:

$$j = \sigma\left[V \cdot B_0 \right]. \quad (3)$$

The numerical modeling of the bias system magnetic field, the eddy current field of the high-frequency inductor [6, 7] and the acoustic field of the EMAT [8-11] was carried out with a purpose of design optimization providing essential conversion efficiency with the current small dimensional parameters of the transducer. The parameters, which were used for optimization, include geometric parameters of the bias system, current parameters of the high-frequency inductor, gaps between the inductor, the bias system and the testing object [7]. The numerical modeling by the finite element technique is realized in software Comsol Multiphysics. Magnet field lines of the bias system of the through-type compressional wave EMAT are illustrated as an example in figure 5.

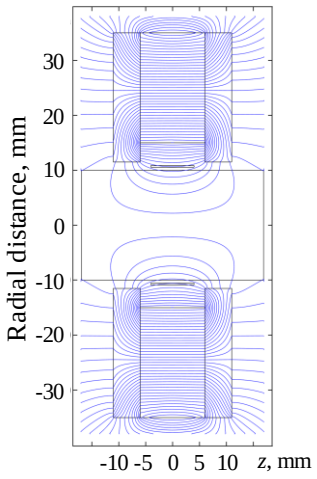

Figure 5. Distribution of the magnetic flux density *B* streamlines of the transducer magnetizing system.

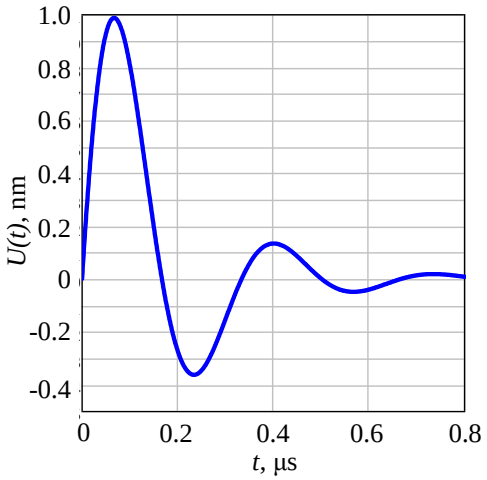

Figure 6. Shape of the displacement pulse $U(t)$ used for solving problem.

The graph of axial B_z magnetic field component distribution on the testing object surface with various values of gaps h between the transducer and the testing object is shown in figure 7 Investigation of these parameters allows defining a width of the high-frequency inductor coiling required for preferred radiation and reception of the compressional waves. Eddy current i_e density distribution under the inductor with various values of the gaps h is shown in figure 8. Values of the axial magnetic field component B_z and surface eddy current density give an opportunity to calculate volume Ampere force density F_{AV} in the area of the object surface layer according to the formula 1 and it is equaled to $2.6 \cdot 10^8$ N/m^3.

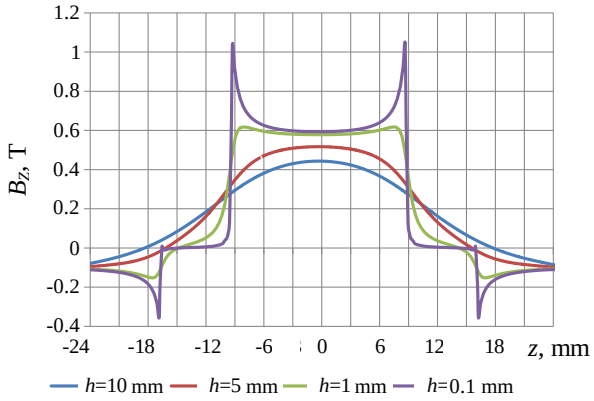

Figure 7. Distribution of the axial B_z magnetic field component on the testing object surface with various values of gaps *h*.

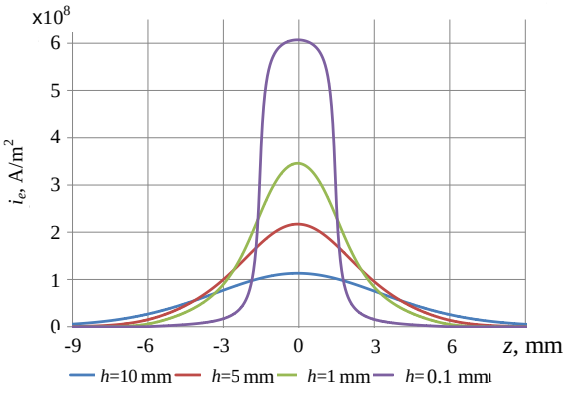

Figure 8. Distribution of the eddy current i_e density under the inductor with various values of the gaps *h*.

When the volume density of Ampere force F_{AV} is known, it is possible to calculate surface density of Ampere force F_{AS} according to St. Venant's principle:

$$F_{AS} = F_{AV} \cdot \Delta \cdot (e-1)/e \approx F_{AV} \cdot 0.632\Delta, \quad (4)$$

where *e* is a base of the natural logarithm.

When the value F_{AS} is obtained, displacement amplitude of the compressional wave U_l generated by the inductor with the surface area *S* can be calculated [12]:

$$U_l = \frac{F_{AS}\, S\gamma^2}{4\pi G\, r}\, j_{l\downarrow}(\theta) e^{-i(\omega t - k_l r)} e^{-k_l h \sin\theta} \frac{\sin(k_l l \sin\theta)}{k_l l \sin\theta}, \quad (5)$$

where F_{AS} is the surface force density [N/m^2], *S* is an inductor surface area in the form of band with current πD_C in length and B_C in width, $\gamma = C_t/C_l$, C_t and C_l are shear and compressional wave velocities in the object, *G* is a shear modulus, $j_{l\downarrow}(\theta)$ is a directivity function of the compressional wave radiated by vertical concentrated force , *h* is a gap between the transducer and the testing object, $k_l = \omega/C_l$ is a wave constant, $\omega = 2\pi f$ is an oscillation circular frequency, θ, *r* are an angle and a distance to the observation point.

In the direction of the radiation maximum θ=0, when *G* = 80 GPa at the distance *r* = 10 mm on the frequency *f* = 2.5 MHz, when the gap is *h* = 1 mm and the surface force density is F_{AS} = 11.7 kN/m^2, the displacement amplitude of the compressional wave is rated as $U_l = 64 \cdot 10^{-12}$ m, which is comparable with piezoelectric transducers by reference to sensitivity.

The result of the acoustic field modeling under the influence of the force action pulse directed tangentially to rod generatrices is illustrated in figure 9 and figure 10.

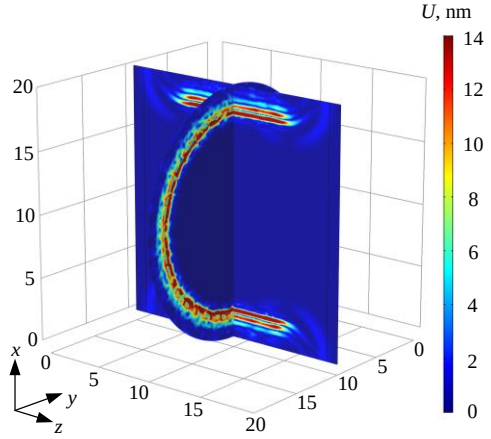

Figure 9. Displacement distribution in the acoustic wave.

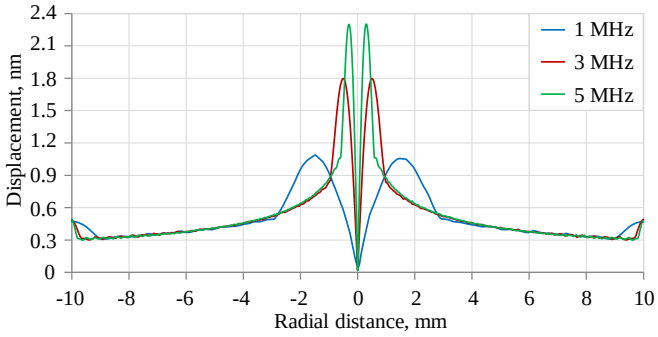

Figure 10. Curves of displacement on various values of frequency.

Acoustic wave propagation front in three-dimensional space is observed as consequence of modeling (figure 9). The wave front in a radial plane of the cross section is spherical convergent, when its shape in an axial plane is close to the shape of plane wave front. Thus, the acoustic wave with cylindrical propagation front is formed in the rod. When wave coming to the rod centre, the increase of the displacement amplitude is observed, and there is focusing of the acoustic oscillations with significant local amplitude increase comparing to the wave amplitude on the surface. Curves of displacement in the compressional wave along the rod diameter are illustrated in figure 10. A focusing factor is defined by a frequency, a rod diameter and probing pulse duration time (figure 6). The highest sensitivity to the small defects located in the central part of the rod is provided on the high values of operating frequency (3-5 MHz); more uniform sensitivity to the defects located at different depths is provided on low values of the operating frequency (1-2 MHz). The developed model also allows getting the multiple reflection series which has great similarities with the real oscillogram (figure 4).

4. Informative parameters of detecting flaws and structural analysis by the mirror through transmission EMA technique

The developed EMA technology is used for detecting flaws of the rods with diameter from 10 to 30 mm and various surface finish quality made by different manufacturers and used for production of extra-weighted pump rods, springs and parts of specialized machinery. Discovered defects of the bar steel rolled stock include nonmetallic inclusions, backfins, decarburized layer, rolled blisters and honeycombs. Pictures of microslices for some types of the obtained defects are given in figure 11 and figure 12. It should be emphasized that crack opening and depth and inclusion sizes are tenth of the acoustic wave length, whereas traditional echo method of ultrasound testing allows detecting defects commeasurable with the wave length.

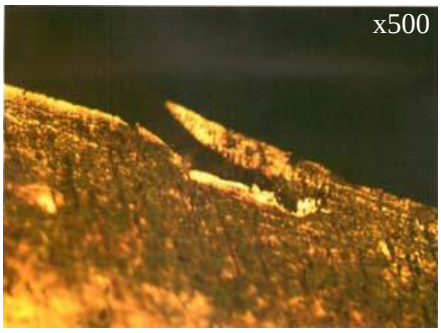

Figure 11. Rolled scab at depth of 0.07 mm, circle 30 mm, steel AISI 9262 (in Russian 60С2ХФА), functional surface finish.

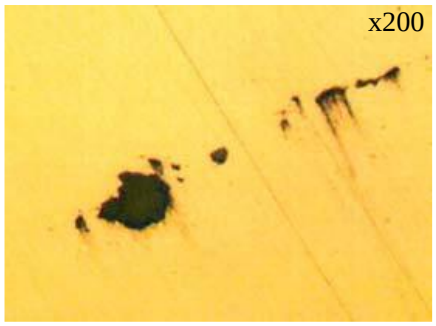

Figure 12. Nonmetallic inclusions 0.05x0.15 mm, circle 21 mm, steel AISI 9262 (in Russian 60С2ХФА), functional surface finish.

A choice of informative parameters and rejection criteria plays an important role during developing the mirror through transmission EMA testing technique. The technique sensitivity to defects and, as a consequence, veracity of testing results depend on competent choice of the informative parameters.

The new approaches to the multiple reflection oscillogram handling based on the correlation, spectral and probability and statistic analyses are suggested by the authors and allowed validating additional informative parameters during the EMA mirror through transmission testing of cylindrical objects. In particular, possibility of object defectiveness degree and defect location depth by means of spectral (figure 13) and such normalized probabilistic characteristics C_n of signal as (mathematical expectation m_x, dispersion D_x, excess E_x, mean square deviation σ_x, asymmetry S_x) (figure 14) is shown.

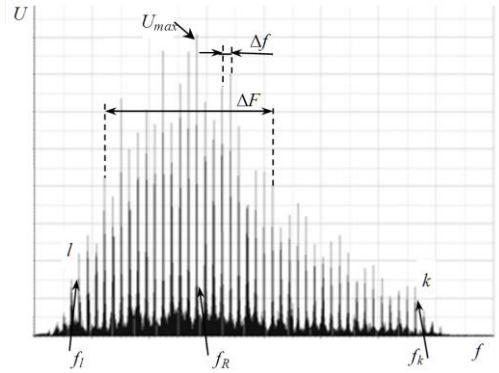

Figure 13. Spectral characteristics of the multiple reflection oscillogram for nondefect sample.

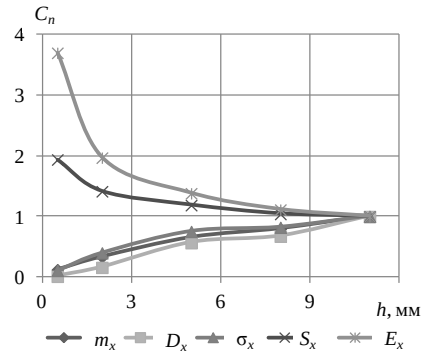

Figure 14. Dependencies of artificial defect location depth influence on the main probabilistic characteristics of the squared signal.

Analysis of volume and Rayleigh wave propagation velocities, attenuation and EMA conversion efficiency for heat-treated samples of bar steel rolled stock made of steel labeled as AISI 5140, AISI 4140, AISI 9262 (in Russian 40X, 40ХГМ and 60С2А respectively) during changing structural state and in the process of mechanical extension is carried out [13]. It is shown, in particular, that the propagation velocities of the compressional, shear and Rayleigh waves have the lowest value in the martensite structure, produced by hardening, with the highest degree of lattice distortion. Further tempering with enhancement and especially softening treatment such as normalization lead to the increase of the ultrasound wave velocity. The volume and Rayleigh wave velocities take the highest values for more equilibrium ferrite-perlitic structures. In grained sorbite the wave velocity has intermediate value.

Mechanical properties (hardness, break point, flaw point and relative elongation) corresponds to structural states of the samples and correlates with the propagation velocities of the shear, compressional and Rayleigh waves (figure 15). The wave velocities is decreasing with the increase of the break and flaw points and the rod hardness and increasing with the increase of ductility and the relative elongation.

When tensile load increasing in elastic area, the linear decrease of the volume and Rayleigh wave propagation velocities is observed. With that, the sensitivity of the shear waves to the mechanical strains is the highest due to coincidence of their axial polarization and applied load direction. The sensitivity to mechanical strains is essentially lower for the compressional and Rayleigh waves with elliptic polarization.

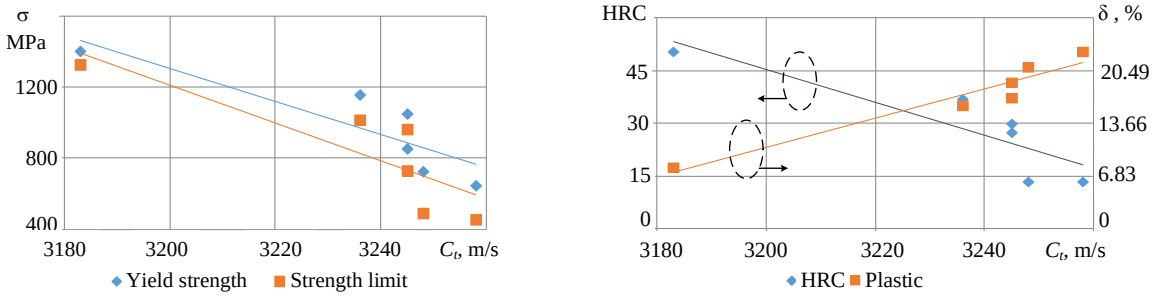

Figure 15. Correlation of the shear wave velocity with mechanical properties of the sample material labeled as steel AISI 5140 (in Russian 40X).

The applicability of the developed EMA technique for estimation of rod cross section geometrical deviation such as ellipticity is shown [14]. In the process of modeling of acoustic wave pulse propagation in the elliptic rod cross section it is shown, that amplitude modulation of the multiple reflection echo-pulses is observed (figure 16), moreover, the higher ellipticity degree, the lower period of amplitude envelope t_e . The shift of the n^{th} pulse of oscillogram for the rod with the ellipticity in reference to the round one is also observed (figure 17). The results of modeling of the multiple reflection series is confirmed experimentally for the rod with round cross section and diameter of 44.0 mm and cross section in the form of ovality with semi-axes of 43.07 and 43.67 mm caused by breaches during rod manufacturing technique.

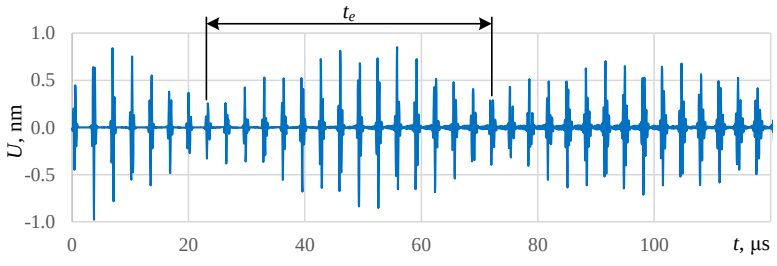

Figure 16. Amplitude modulation of multiple reflection oscillogram when ellipticity is equal to Δ = 0.15 mm (rod diameter is 20 mm, the EMAT operating frequency is 3 MHz).

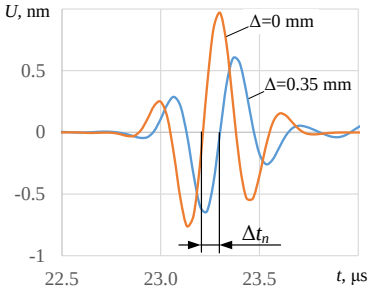

Figure 17. The shift of the n^{th} pulse for the rod with ellipticity in reference to the round rod.

5. Conclusions

The results of numerical modeling of the magnetic, eddy current and acoustic EMA transducer fields allow estimating displacement amplitude in the radiated wave and validating the best construction providing the greatest possible conversion efficiency and preferred radiation-reception of one main type of wave by the transducer; setting requirements to the main technique parameters in order to reach the highest value of the sensitivity to defects.

The suggested approaches to the numerical processing of the multiple reflection oscillograms based on the spectral and probability and statistic analyses allow validating additional informative parameters of the EMA mirror through transmission testing technique of cylindrical objects.

The developed noncontact EMA technique of the mirror through transmission method on multiple reflections using compressional, shear and Rayleigh waves shows the high sensitivity to internal and surface defects of bar steel rolled stock and is applicable for estimating elastic properties, heat-treatment quality, structural state and stress-strain behavior of rods.

The developed testing technique has the following advantages: realization of the method without immersion liquid and additional surface preparation providing sufficiently high control efficiency; high veracity and repeatability; absence of ‘dead zone’; the applicability of techniques for testing rods made of various metals and alloys.

Acknowledgments

The reported study was funded by Russian Science Foundation according to the research project №15-19-00051.

References

[1] Hirao M and Ogi H 2003 *EMATS for science and industry: noncontacting ultrasonic measurements* (Boston: Kluwer Academic Publishers)
[2] Watson N J, Hazlehurst T, Povey M J W, Drennan A and Seaman P 2015 *J. Phys.: Conf. Ser.* **581** 012008
[3] Babkin S E 2015 *Russian Journal of Nondestructive Testing* **51** pp 303-07
[4] Muravev V V, Muraveva O V, Strizhak V A, Pryakhin A V and Fokeeva E N 2014 *Russian Journal of Nondestructive testing*, **50** 435-442
[5] Strizhak V A, Priahin A V, Obuhov S A and Efremov A V 2011 *Intellectualnie systemi v proizvodstve* **1** 243-250
[6] Ashigwuike E C, Ushie O J, Mackay R and Balachandran W 2015 *Sensors and Actuators A: Physical* **229** 154-165
[7] Muravieva O V, Petrov K V and Myshkin Yu V 2016 *IEEE Industrial Engineering, Applications and Manufacturing (ICIEAM), International Conference on* **1** 1-4
[8] Nakahata K, Kawamura G, Yano T and Hirose S 2015 *Construction and Building Materials* **78** 217-223

[9] Xie Y, Rodriguez S, Zhang W, Liu Z, and Yin W 2016.*Ultrasonics* **66** 154-165
[10] Petrov K V, Muravieva O V and Gabbasova M A 2017 *J. Phys.: Conf. Ser.* **803** 012114
[11] Xie Y, Rodriguez S, Zhang W, Liu Z, and Yin W 2016 *Journal of Sensors* **2016** 5451821
[12] Budenkov G A, Nedzvetskaia OV 2004 *The dynamic problems of elastic theory in application to the problems of acoustic testing and diagnostics* (Moscow: Physmatlith) p 136
[13] Muravieva O V, Muraviev V V, Gabbasova M A, Petrov K V and Zorin V A 2016 *Mechanics, Resource and Diagnostics of Materials and Structures (MRDMS-2016)* vol 1785 ed E S Gorkunov, V E Panin and S Ramasubbu (Ekaterinburg: AIP Conf. Proc.) 030017
[14] Muravieva O V, Petrov K V, Sokov M Y and Gabbasova M A 2015 *Russian Journal of Nondestructive Testing* **51** 400−06